A comparison of the theoretical and experimental results for keV electron scattering from argon

M Vos[1], R P McEachran[1] and Lin-Fan Zhu[2]

[1] Atomic and Molecular Physics Laboratories, Research School of Physics and Engineering, Australian National University, Canberra, ACT 0200, Australia
[2] Hefei National Laboratory for Physical Sciences at Microscale, Department of Modern Physics, University of Science and Technology of China, Hefei, Anhui 230026, People's Republic of China

E-mail: Maarten.Vos@anu.edu.au

Abstract

Experiments studying the scattering of keV electrons from noble gas atoms have been performed in the past, as the first Born approximation (FBA) was thought to be valid under these conditions, and hence it was expected that these experiments could be modelled relatively straightforwardly by theory. Somewhat surprisingly these experiments have so far attracted only very limited theoretical interest and the ability of modern scattering theory to describe them has not been firmly established. In our earlier study of the cross section for the resonant transitions, we established that the FBA was sufficient to describe the results for small scattering angles, but it did not account for the observed intensity at larger angles. Here we extend this comparison for the case of argon to monopole, quadrupole and octopole transitions below the continuum. The experimental results show differential cross sections spanning many orders of magnitude for these transitions. The relativistic distorted wave theory developed here describes these experiments for many transitions and a large range of scattering angles reasonably well.

Keywords: electron scattering, argon, generalized oscillator strength, relativistic distorted wave

(Some figures may appear in colour only in the online journal)

1. Introduction

Electron scattering from noble gases has been studied for about a century, and has been seen for a long time as a 'simple test case' of our understanding of the interaction of electrons with matter. The subject has been thoroughly reviewed recently [1] for the case of Ar. In spite of the experimental and theoretical efforts spanning decades, our understanding is still rather rudimentary. For example, the quoted error bars of the optical oscillator strengths (OOSs), as derived from experiments, are much smaller than the variation between the values obtained from different experiments. The variation in the calculated OOSs, as obtained by different theories is large as well. Thus even for the most basic quantities our understanding is still unsatisfactory.

It is thus desirable to revisit this problem and focus on conditions where agreement between theory and experiment should be most easily obtained. Electron scattering at high energies (incoming energy E_0 above one keV) is such a case, as the first Born approximation (FBA) was expected to be very good under these conditions. Such consideration has led to a number of high-quality measurements of electron scattering at 2500 eV [2–6] and at slightly lower energies (300–500 eV) [7–9].

Theoretical interpretation has concerned itself with the shape of the spectra, exploring the difference in shapes of the generalized oscillator strength (GOS) for monopole, dipole and quadrupole transitions [10–12]. These papers use the FBA, and explore the influence on the GOS of electron–electron correlation beyond a mean-field approach. The overall shape
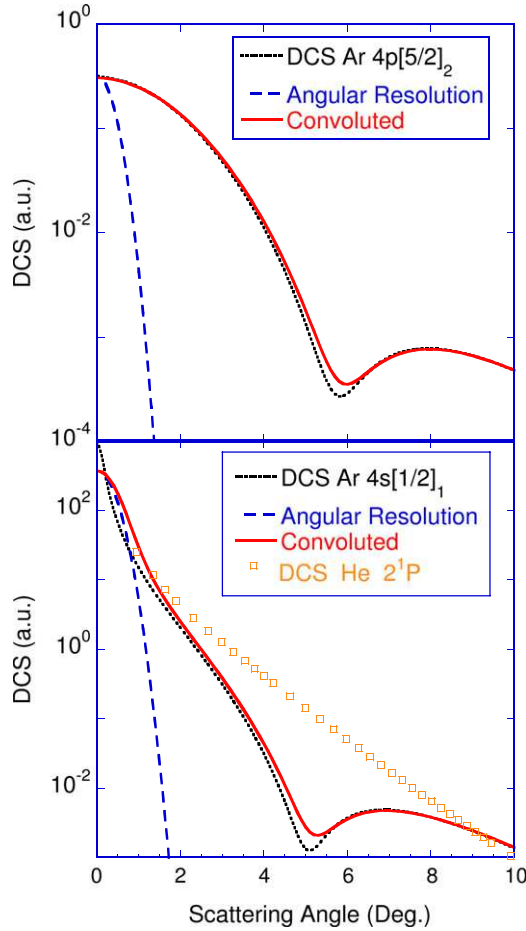
Figure 1. An estimate of the effect of finite angular resolution on the measurements. The theory (dots) is convoluted with a Gaussian of 0.8° FWHM (dashed line), and the result is plotted as a full line. For the (dipole-allowed) $4s[1/2]_1$ transition the deviation is strong at small angles ($\theta < 2°$) and at the minimum near 6° (corresponding to $K \approx 1.4$ au). For the (quadrupole) $4p[5/2]_2$ transition the influence of the finite angular resolution is only visible near the minimum at 5° ($K \approx 1.2$ au). In the bottom panel we also show the DCS for the 2^1P transition of He, corresponding to the GOS, as published by Cann and Thakkar [27], which was used to put the cross section on an absolute scale.

of the GOS curves turns out to be a clear signature of the difference in angular momentum of the initial and final states, and the amplitude of the GOS is affected by electron–electron correlations.

Experimentally there was measurable intensity for large scattering angles, even at 6 keV [13], in contrast to expectations based on the FBA. A breakdown of the FBA at large momentum transfer was also evident from a comparison of electron and x-ray scattering results for scattering from N_2 [14]. Such intensity was reproduced successfully by the relativistic distorted wave (RDW) theory (which goes beyond the FBA) which for Ar and Ne gave quite a good quantitative description for the intensity of the resonant transitions [15], even at very high momentum transfer (up to ≈ 20 au). For Ne the RDW theory was used to simulate the spectra up to the onset of the continuum, and the level of agreement was mixed; in particular the quantitative description of the monopole transitions presents a significant challenge [16]. In

this paper we want to study the case of Ar in a similar way using both high energy resolution measurements at low and intermediate momentum transfer and lower energy resolution measurements at higher momentum transfer.

2. Theory

Here the inelastic differential cross sections and GOSs were calculated using the RDW method. Within the FBA the GOS is only a function of the transferred momentum. The RDW method goes beyond the FBA and the GOS becomes a function of both the transferred momentum and the energy of the probing electron. For this reason one refers to the GOS under conditions that the FBA does not apply as an 'apparent GOS'. This method has been described in detail in [15] and hence only a brief outline of the method is presented here.

In intermediate coupling notation, the excited states of a noble gas are denoted by $n'\kappa'[K]_J^P$. The total differential cross section $\sigma_{n'\kappa'}^{JK}(\hat{\boldsymbol{k}}_b)$ for the excitation of this state from the ground state is then given by

$$\sigma_{n'\kappa'}^{JK}(\hat{\boldsymbol{k}}_b) = \frac{1}{2} \sum_{M=-J}^{J} \sum_{\mu_a \mu_b} \left| f_{n'\kappa'}^{JK}(M, \mu_a, \mu_b; \hat{\boldsymbol{k}}_b) \right|^2 \qquad (1)$$

where $f_{n'\kappa'}^{JK}(M, \mu_a, \mu_b; \hat{\boldsymbol{k}}_b)$ is the scattering amplitude which is given in terms of the corresponding T-matrix element by

$$f_{n'\kappa'}^{JK}(M, \mu_a, \mu_b; \hat{\boldsymbol{k}}_b) = (2\pi)^2 \left(\frac{k_b}{k_a} \right)^{\frac{1}{2}} T_{n'\kappa'}^{JK}(M, \mu_a, \mu_b; \hat{\boldsymbol{k}}_b). \tag{2}$$

In the above equations J and M are the total angular momentum quantum numbers of the excited state, μ_a, μ_b are the magnetic spin projection quantum numbers of the incident and outgoing electrons while $\hat{\boldsymbol{k}}_a$, $\hat{\boldsymbol{k}}_b$ denote the directions of the incoming and outgoing electrons. The angular momentum quantum number κ is defined in terms of the orbital and total angular momentum quantum numbers (l, j) of an electron by $\kappa = -l - 1$ for $j = l + \frac{1}{2}$ while $\kappa = l$ for $j = l - \frac{1}{2}$.

The T-matrix elements in equation (2) are expressed in terms of the RDWs as follows:

$$T_{n'\kappa'}^{JK}(M, \mu_a, \mu_b; \hat{\boldsymbol{k}}_b) = \langle \phi_b \left(n'\kappa'[K]_J^P \right)$$
$$\times F_{b\mu_b}^-(\boldsymbol{x}, \sigma) | V - U | \mathcal{A} \{ \phi_a(00) \, F_{a\mu_a}^+(\boldsymbol{x}, \sigma) \} \rangle. \tag{3}$$

Here $\phi_a(00)$ is the ground state Dirac–Fock (DF) wavefunction with $J = M = 0$ which was determined in a separate DF calculation using just a single configuration while $\phi_b(n'\kappa'[K]_J^P)$ is the excited state wavefunction with total angular momentum quantum numbers J and M, and P is the parity of the state. These wave functions are calculated in a multiconfiguration procedure. Furthermore, $\mathcal{A}$ is the antisymmetrization operator, $F_{a\mu_a}^+(\boldsymbol{x}, \sigma)$ and $F_{b\mu_b}^+(\boldsymbol{x}, \sigma)$ are RDWs, V is the total interaction potential between the incident electron and the atom while U is the so-called distortion potential. Here $(\boldsymbol{x}, \sigma)$ are the space and spin coordinates of the incident electron. Explicit expressions for all these wavefunctions and the RDWs as well as the above potentials can be found in equations (5)–(9) of [15]. The DF wavefunctions of the argon atom were determined using the MCDF program of Grant *et al* [17].
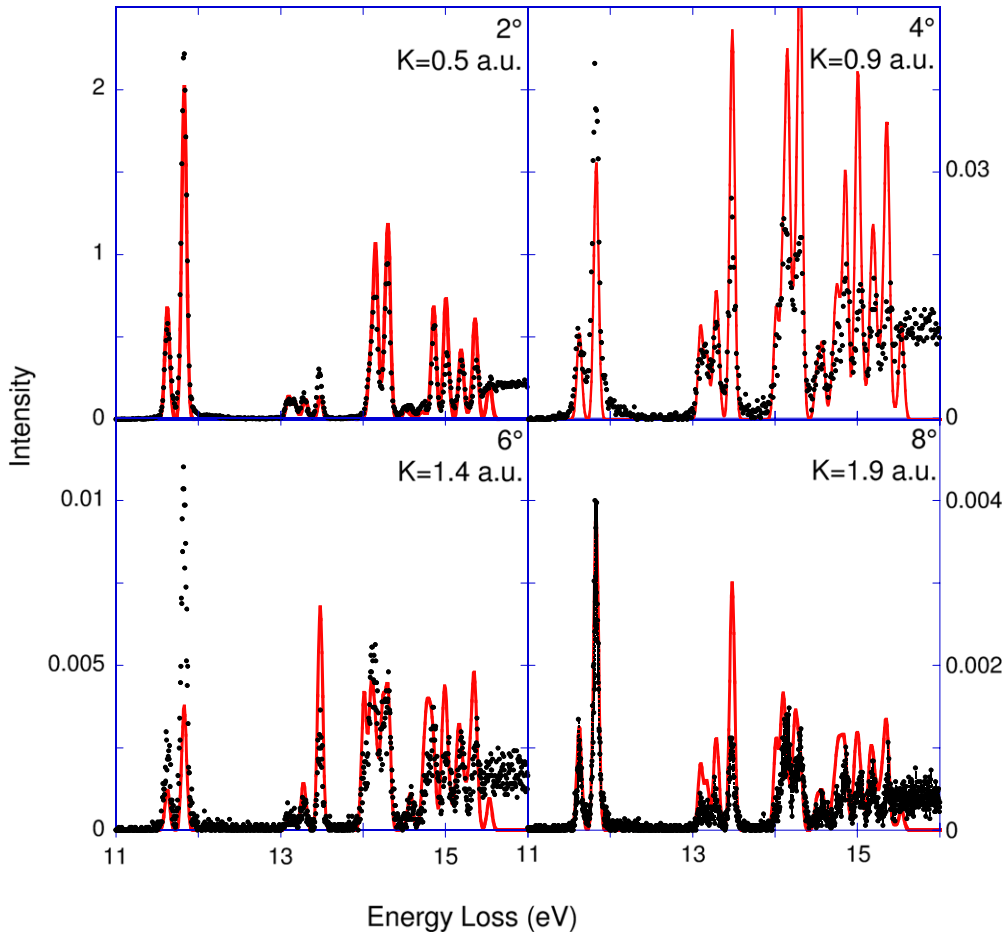
Figure 2. Spectra taken at angles as indicated, compared to the calculated intensity broadened by the experimental energy resolution.

Finally, the GOS for a given excited state can be expressed in terms of the corresponding differential cross section according to

$$f(E_b, K^2) = \frac{E_b}{2} \frac{k_a}{k_b} K^2 \, \sigma_{n'\kappa'}^{JK}(\hat{\boldsymbol{k}}_b) \qquad (4)$$

where $K = |\boldsymbol{k}_b - \boldsymbol{k}_a|$ is the momentum transfer and E_b the excitation energy. The OOS can then be found from the following limit:

$$f_{b \leftarrow a} = \lim_{\substack{K^2 \to 0 \\ k_a^2 \to \infty}} f(E_b, K^2). \qquad (5)$$

Our calculated OOS values are compared in table 1 with previously published ones. As stated before there is a considerable spread in the OOS values obtained by various authors for these dipole-allowed transitions.

The elastic differential cross section for the ground state of argon was determined using the relativistic optical potential (ROP) method of Chen *et al* [18]. This optical potential is complex, with the real part describing the static and polarization interactions of the target atom with the incident electron while the imaginary part describes the loss of incident flux into excitation and ionization channels. As in [15], we use a local polarized-orbital polarization potential, which contained six static multipoles and up to five dynamic terms. The precise form of the static potentials is discussed in [19] while the dynamic potentials are discussed in [20] and applied to argon in [21–23].

Table 1. Optical oscillator strengths as obtained in this work (RDW), calculated for $E_0 = 4$ keV, compared to the values given by Zatsarinny and Bartschat (ZB) [25], Gargioni and Grosswendt (GG) [1] and by Verner *et al* (VVF) [26].

State	E (eV)	RDW	ZB	GG	VVF
4s[3/2]$_1$	11.624	0.0736	0.0640	0.060	0.0665
4s[1/2]$_1$	11.828	0.222	0.242	0.233	0.244
3$\bar{\text{d}}$[1/2]$_1$	13.864	0.000 65	0.000 95	0.00102	–
5s[3/2]$_1$	14.090	0.0331	0.0320	0.0257	0.0268
3d[3/2]$_1$	14.153	0.125	0.0895	0.083	0.0930
5s[1/2]$_1$	14.255	0.0255	0.0170	0.0110	0.0119
3$\bar{\text{d}}$[3/2]$_1$	14.304	0.128	0.0746	0.092	0.106
4$\bar{\text{d}}$[1/2]$_1$	14.711	0.000 16	0.0016	0.0019 [24]	–
6s[3/2]$_1$	14.848	0.0138	0.0127	0.0144 [24]	–
4d[3/2]$_1$	14.859	0.0649	0.0468	0.0484 [24]	–
4$\bar{\text{d}}$[3/2]$_1$	15.004	0.0711	0.0040	0.0209 [24]	–
6s[1/2]$_1$	15.022	0.00807	0.0317	0.0221 [24]	–
5$\bar{\text{d}}$[1/2]$_1$	15.118	7.8×10^{-5}	–	0.0041 [24]	–
7s[3/2]$_1$	15.186	0.00688	}0.0361	–	–
5d[3/2]$_1$	15.190	0.0381		0.0426 [24]	–

The imaginary part of the potential (representing absorption) was determined as an expansion over the inelastic channels of the target atom. These inelastic channels included both excitation of the higher lying bound states as well as single ionization of the target as given by equation (21b) of [18]. In particular, 14 bound state and 27 continuum state channels
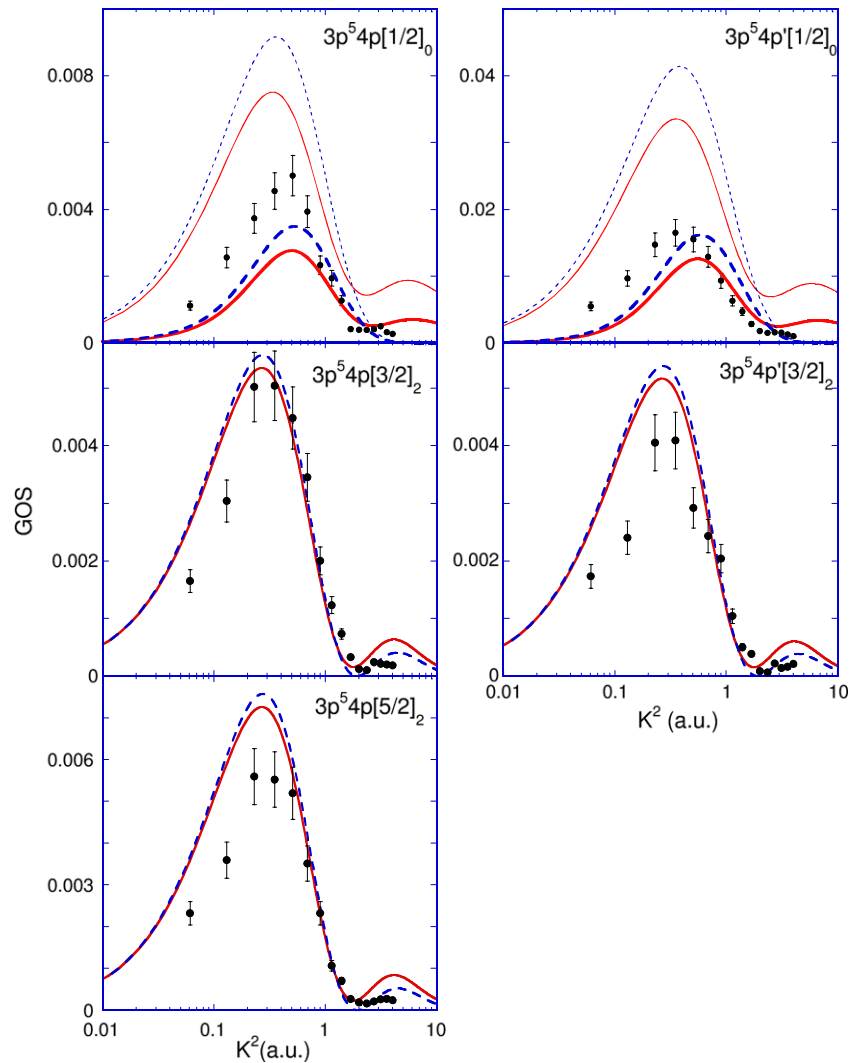
Figure 3. Measured (dots) and calculated GOS for several monopole and quadrupole transitions of Ar. The calculated GOS curves are given for the FBA (dashed line) and the RDW theory (full line). For the monopole transitions there are thick and thin lines, corresponding to calculations following the DCS1 and DCS2 schemes respectively, as described in the text.
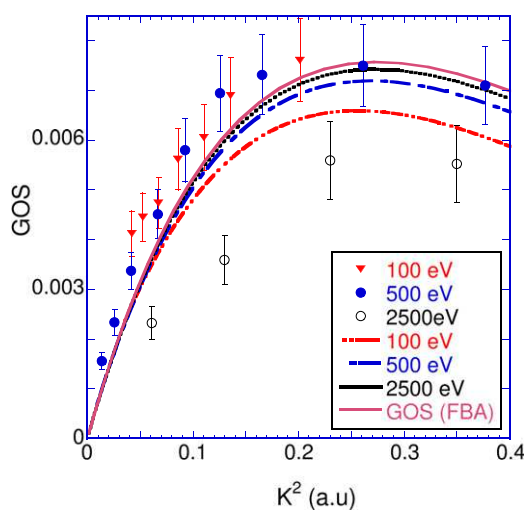

Figure 4. GOS curve for the $4p[5/2]_2$ transition at relative small K^2 values as measured by Suzuki *et al* (at 100 and 500 eV) [9] and Zhu *et al* at 2500 eV [3] (symbols). The measurements are compared to the present RDW calculations at the corresponding energies as indicated as well as a FBA calculation (lines).

were included where either a $3\bar{p}$, 3p or 3s electron was ionized. The precise details of which states were included can be found in [15]. Once again, the bound state DF wavefunctions of the target atom were calculated using the MCDF program of Grant *et al* [17] while the scattering wavefunctions and elastic differential cross sections were determined in accordance with equations (11)–(14) of [15].

Both the RDW and ROP methods described above are based upon the use of the Dirac Hamiltonian. It should be noted however, that the relativistic effects which arise in these methods are due to the speed of the inner shell electrons of the target atom being a significant fraction of the speed of light. Apart from spin there are very minimal relativistic effects associated with the incident electrons at these relatively low energies.

3. Experimental details

As most of the experimental results have been published before we only give a very brief summary here. The small-angle scattering experiment uses a monochromatized electron beam
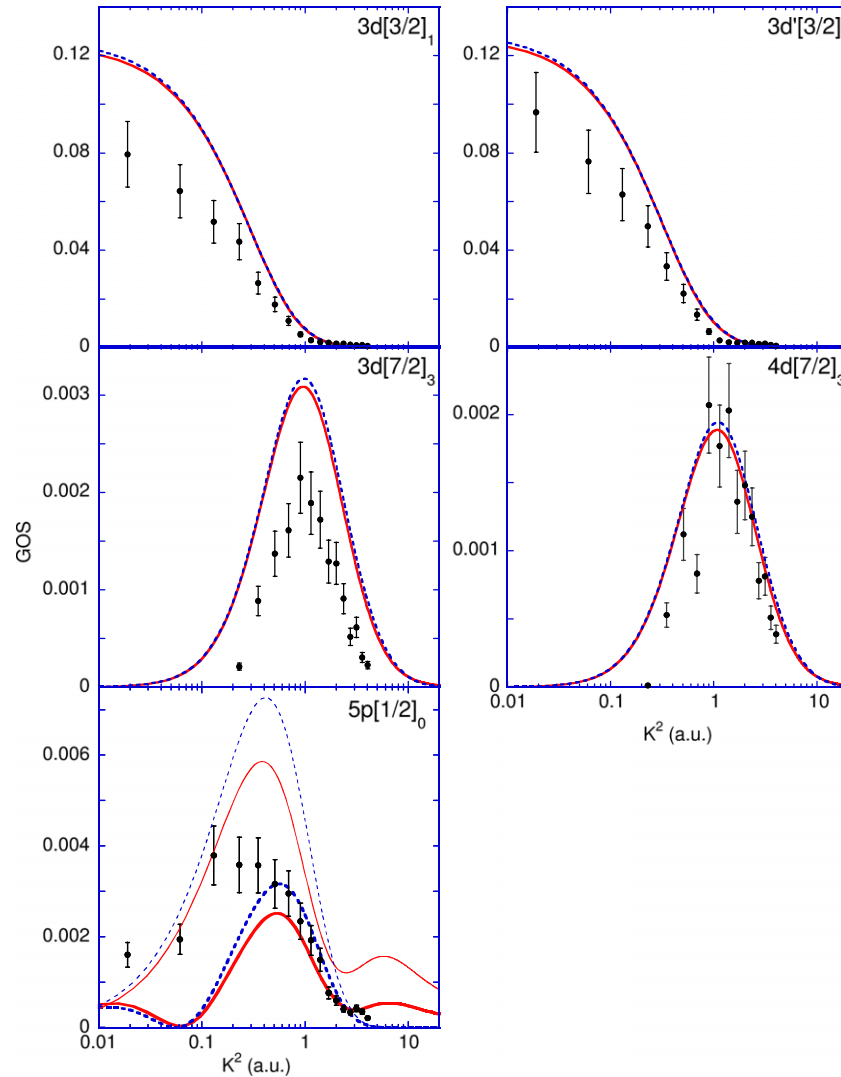
J. Phys. B: At. Mol. Opt. Phys. **47** (2014) 055201

M Vos *et al*

Figure 5. Same as for figure 3, but for some deeper levels.

with an energy of 2500 eV and a gas cell [3]. The energy resolution is 75 meV full-width at half-maximum (FWHM), and the angular resolution is 0.8° FWHM. In order to get the spectra on an absolute scale a mixture containing a fixed amount of He is used, and the spectra are normalized using the He 2^1P peak and the known GOS of this level as well as the OOS of the $4s[1/2]_1$ state of argon [27]. In a second spectrometer [15] we use an unmonochromatized BaO source as an emitter and scattering angles of either 45°, 90° or 135°. This spectrometer has an energy resolution of 0.3 eV FWHM. The elastic peak is included in these measurements as well, and the loss part of the spectrum is set on an absolute scale using the calculated elastic scattering cross section for these conditions.

Before we start discussing the obtained GOSs, it is worthwhile emphasizing that the actual measurements are of the differential cross sections. The relation between the GOS and the DCS is given in equation (4). If the GOS values are relatively constant at small scattering angles, the actual DCS diverges as $1/K^2$. Under these conditions the angular resolution of the experiment has a significant influence on the outcome. The matter is complicated by the fact that we use the He 2^1P transition to put the experiment on an absolute scale. This transition also has a strong angular dependence of the cross section. Dipole-allowed and dipole-forbidden transitions behave completely differently at small scattering angles, hence these angular resolution effects can distort the spectrum significantly, especially at relatively small scattering angles. This is illustrated in figure 1. These plots also underline that the actual observable (the DCS) varies by up to a factor of 10^5 in these experiments. The agreement between experiment and theory should be judged keeping this huge variation of the DCS in mind as well as the limited angular resolution.

4. Results

In figure 2 we show a selection of the high energy resolution spectra of the experiment described in [3, 4] at the angles as indicated. The measured spectra are compared with the calculated intensity convoluted with the experimental resolution of 75 meV. Both the measured and calculated intensity decrease by several orders of magnitude with
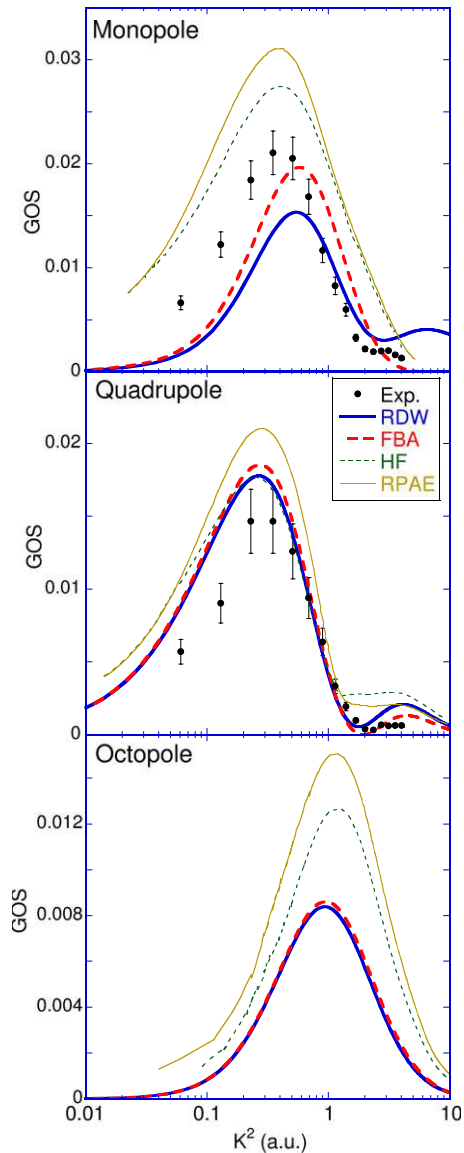
J. Phys. B: At. Mol. Opt. Phys. **47** (2014) 055201

M Vos *et al*

Figure 6. A comparison of the combined intensity of the 3p → 4p quadrupole (top) and the 3p → 4p monopole transitions (bottom) with the corresponding calculated intensity of the present work (labelled RDW and FBA as well as those published by Amusia (labelled HF and RPAE). The bottom panel shows the 3p → 3d octopole transitions. Here the experiment is absent as some of the octopole transitions cannot be separated from other transitions.

increasing angle, but substantial differences between theory and experiment exist as well.

A comparison of the intensity distribution of the GOS for the resonant (3p → 4s) transitions between 11 and 12 eV was given in [15]. Deviations between theory and experiment are here substantial (a factor of 3) near the minimum in the GOS at 1.4 au. The limited angular resolution is for a large part responsible for the filling in of the minimum (see figure 1). At both the highest and lowest momentum transfers shown (0.5 and 1.9 au) the agreement is good for the resonant transitions. The second group of transitions (between 13 and 13.5 eV energy loss) are due to 3p→4p transitions. These levels are fairly well resolved and extracting the GOS from the experiment is straightforward. The next

group between ≈ 13.9 and 14.2 eV are 3p→3d transitions as well as 3p→5s transitions. The levels become more closely spaced with increasing energy and extracting their intensity relies on careful curve fitting, as was described in [4], but even then some levels are too close in energy to be separated.

Let us first compare the GOS as obtained from these measurements with the calculated ones for the 3p→4p transitions. These are either monopole or quadrupole transitions and they are compared with the calculated GOS values in figure 3. Experimentally the monopole transitions peak at slightly larger K^2 values than the quadrupole ones and this is replicated by theory.

There are some complications in the calculation of the intensities for the monopole transitions where the excited state wavefunction has the same angular momentum quantum numbers ($J = M = 0$) as the ground state as explained in [16]. In these cases, the ground and excited state wavefunctions will not be automatically orthogonal if they are obtained in separate MCDF calculations. This difficulty was overcome in two different ways. First, the ground and excited state wavefunctions were determined in the *same* MCDF calculation. We will denote our results obtained in this manner as DCS1. Alternatively, the ground and excited state wavefunctions which were determined in separate MCDF calculations were then orthogonalized using the Gram–Schmidt procedure. We will denote our results obtained in this manner as DCS2.

For the monopole transition the agreement is less good, but the experimental observation is in between calculations based on the DCS1 and DCS2 schemes. The cause of the disagreement is thus most likely in the shortcomings of the orthogonalization procedure. However, the difference between the FBA and RDW theories are also more substantial for the monopole compared to the quadrupole transition. The monopole cross section is thus also sensitive to the details of the incoming and outgoing wavefunctions of the probing electron.

Agreement between the present RDW calculation and the experiment is better for the quadrupole transitions, where the aforementioned orthogonalization problem does not exist. The position of the maximum is well described by the theory and GOS value at this maximum deviates from the experimentally observed one by less than 20%. However, on the low momentum side of the main peak the experimental intensity decreases more quickly than the calculated one for all three levels. This could be a consequence of the normalization procedure used, as for small momentum transfer values the He 2^1P transition intensity (used in the normalization procedure) decreases very rapidly with increasing scattering angle [28]. Due to the finite opening angle of the spectrometer, the effective scattering angle for the He 2^1P transition could be somewhat smaller, and hence its intensity could be increased relative to the calculated intensity assuming an infinitely small opening angle. The differences between the FBA and RDW intensities are small for these quadrupole transitions in the momentum range plotted.

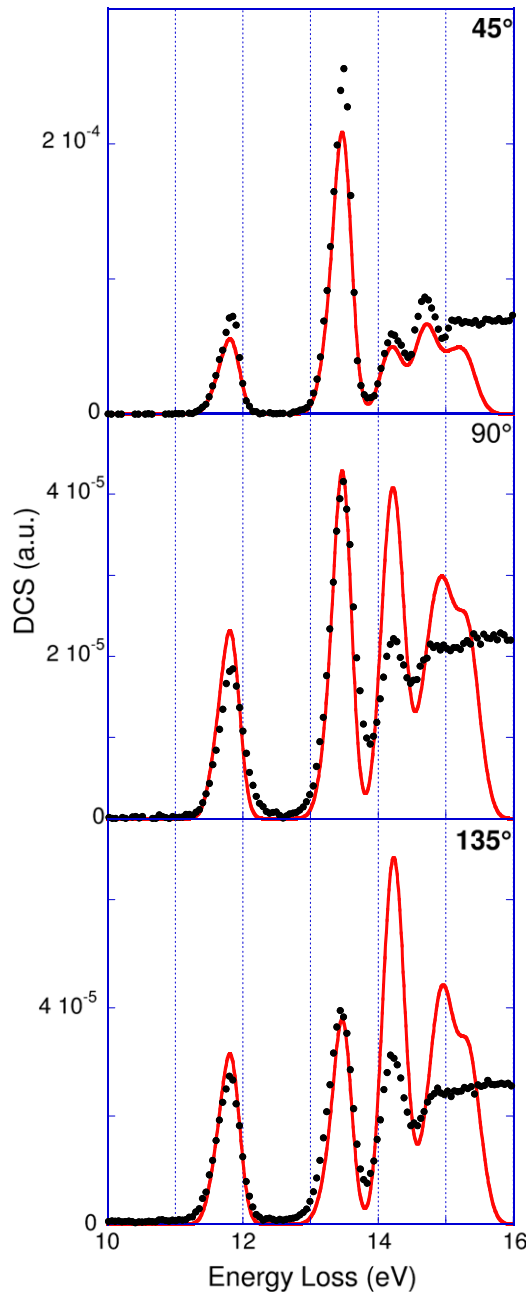Suzuki and co-workers studied the onset at low momentum transfer of the GOS of these quadrupole transitions

Figure 7. Measured spectra at large scattering angles (45°, 90°, 135°), taken at 1 keV, compared with theory. The experiment is normalized to the theory using the elastic peak (not shown).

Figure 8. The top panel shows how the calculated intensity (using the RDW theory, expressed as a fraction of the elastic DCS) for the various 4p excitations develops as a function of the scattering angle. The lower panel compares the measured ratio (summed over for all $3p \rightarrow 4p$ excitations) with the calculated one. The same comparison is made for the $3p \rightarrow 4s$ excitations. All plots are for $E_0 = 1$ keV.

in greater detail [9] at somewhat lower energies (100–500 eV). In figure 4 we compare their experimental data for the onset of the main peak with those of [3] and the RDW theory at the corresponding energies for the $4p[5/2]_2$ transition. With increasing energy of the incoming particles the distortion effects become less severe and the RDW result merges with the FBA result in the high energy limit as is shown in figure 4. The present calculation is closer to the data taken at lower incoming energies. Somewhat disappointingly, the trend in the RDW calculations (increase in GOS values with increasing electron energy) is the opposite of the trend seen in the experiment.

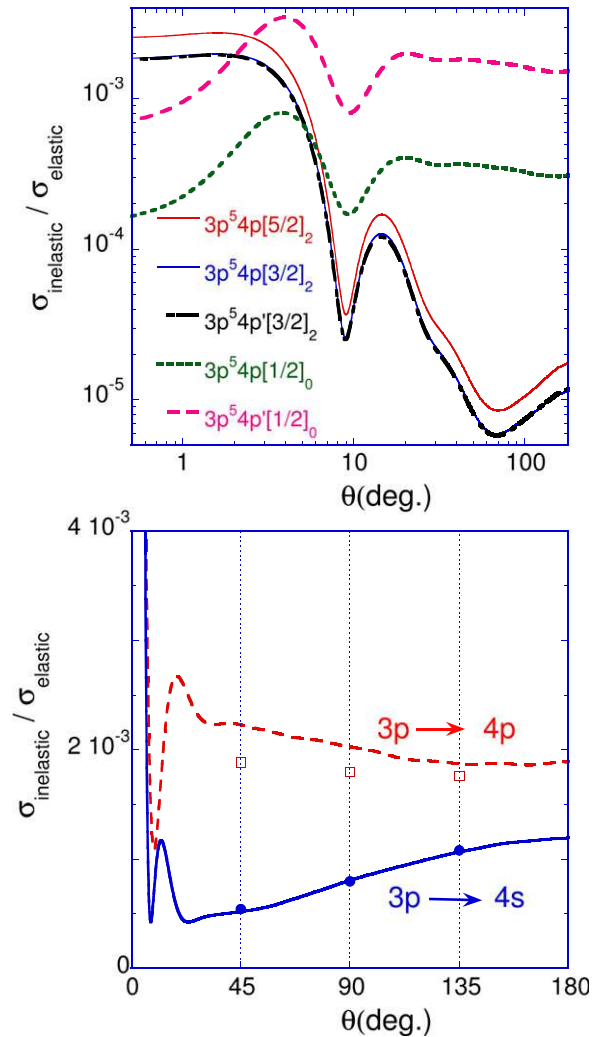Similar comparisons were made for some of the deeper levels, in particular those levels for which the GOS was obtained in [4], see figure 5. The overall shape of the GOS for dipole transitions involving a 3d final state is well reproduced by theory, but the intensity seems somewhat too large. Two octopole transitions are shown, one involving 3d and one involving 4d electrons. There is good agreement in shape, but the calculated intensity is somewhat larger. The monopole transition again has a difference of a factor of 2 between the DCS1 and DCS2 approaches, with the measured GOS being again in between the two calculations.

In figure 6 we compare the total GOS curves for the sum of the $3p \rightarrow 4p$ monopole and of the sum of the $3p \rightarrow 4p$ quadrupole transitions as well as of the sum of the $3p \rightarrow 3d$ octopole transitions with the results of Amusia *et al* [10–12]. For the monopole and quadrupole transitions the calculations are also compared to the experiment [3], but for two of the three $3p \rightarrow 3d$ octopole transitions there is an overlap with dipole-allowed transitions with much bigger intensity, which makes the comparison not meaningful [4]. Only for the quadrupole is

there good agreement between the FBA (DF) theory described here, and the FBA (Hartree–Fock) theory of Amusia.

We now shift our attention to the lower energy resolution spectra taken at larger momentum transfer. Here the FBA predicts virtually no intensity. In [15] we showed that the shape of the loss spectrum changes with scattering angle, and its intensity relative to the elastic peak decreases approximately proportional to $1/E_0$. Now we use the RDW theory to generate a complete spectrum, assuming an experimental resolution of 300 meV, and this spectrum is shown in figure 7. Here we use the elastic peak (included in the measurement as well, but not shown in figure 7) to put the experiment and the theory on the same intensity scale, using the elastic scattering program from Chen *et al* [18]. The agreement between the measured and calculated spectrum is very good for the 3p→4s and the 3p→4p parts of the spectrum, and somewhat less good for the deeper levels. It is interesting to plot the angular dependence of the intensity of the various (here non-resolved) 3p→4p transitions. This is performed in figure 8. Interestingly for the 3p→4p transitions the quadrupole intensities decrease much more dramatically than the monopole intensities. At large scattering angles the intensity of the 3p→4p region is almost exclusively due to monopole transitions. The angular dependence of the dipole transitions is shown as well. Its intensity (expressed as a fraction of the elastic peak) increases with θ for large scattering angles, whereas the monopole transition shows a slight decrease with θ at large scattering angles.

5. Discussion and conclusions

In recent times there have been two theoretical approaches of describing these electron scattering experiments at keV energies. The approach of Amusia and co-workers employs the FBA but describes electron–electron correlation beyond the mean-field approximation. The RDW approach, used here, avoids the assumption of plane waves for the scattering electron by using distorted waves, but in this case there is no attempt made to treat the electron–electron interaction beyond a mean-field model.

For large angle scattering of keV electrons it is clear that RDW-type corrections on the FBA are required to reproduce the significant intensity observed in the experiments. At small momentum transfer there appears to be significant influence on the GOS of distortion for monopole transitions, whereas its effect for dipole, quadrupole and octopole transitions is minor.

At smaller scattering angles we obtain good agreement within the FBA for quadrupole transitions between our DF theory and the HF theory of Amusia *et al* but not for the monopole and octopole transitions. Disagreement for a FBA calculation for either a DF of HF theory seems to indicate that the quality of the wavefunctions used in these theories is causing similarly sized discrepancies as the correlation effects seen in the RPAE. For the DF theory described here this applies even to the monopole transitions where different orthogonalization procedures lead to rather different results. Only when there is consensus on the calculated GOS of different theories *within* a mean-field theory, do we have any

hope of studying correlation effects by comparing calculations that go beyond a mean-field description of the target with experiments.

Thus the 'simple' problem of inelastic excitations due to electron scattering at keV energies from argon still has many open-ended questions. The most interesting one could well be if we can identify correlation effects on the GOS distribution. This requires firstly agreement between different approaches on the mean-field values of the GOS curves. Measurements with better angular resolution would also greatly facilitate the comparison of theory with experiment, especially when the DCS varies over several orders of magnitude.

References

[1] Gargioni E and Grosswendt B 2008 Electron scattering from argon: data evaluation and consistency *Rev. Mod. Phys.* **80** 451–80

[2] Fan X W and Leung K T 2000 Absolute generalized-oscillator-strength measurement of preionization-edge electronic excitations in the valence and 2p shells of argon *Phys. Rev.* A **62** 062703

[3] Zhu L-F, Cheng H-D, Yuan Z-S, Liu X-J, Sun J-M and Xu K-Z 2006 Generalized oscillator strengths for the valence-shell excitations of argon *Phys. Rev.* A **73** 042703

[4] Zhu L-F, Yuan H, Jiang W-C, Zhang F-X, Yuan Z-S, Cheng H-D and Xu K-Z 2007 Generalized oscillator strengths for some higher valence-shell excitations of argon *Phys. Rev.* A **75** 032701

[5] Yuan Z-S, Sakai Y, Umeda N, Fujita Y, Takayanagi T, Yamada C, Nakamura N, Ohtani S, Zhu L-F and Xu K-Z 2006 Autoionization states in xenon investigated by electron impact *J. Phys. B: At. Mol. Opt. Phys.* **39** 5097–103

[6] Zhu L-F 2010 The valence shell excitations for some noble atoms studied by fast electron impact *J. Phys.: Conf. Ser.* **235** 012007

[7] Suzuki T Y, Suzuki H, Ohtani S, Min B S, Takayanagi T and Wakiya K 1994 Measurements of cross sections and oscillator strengths for ne by electron-energy-loss spectroscopy *Phys. Rev.* A **49** 4578–84

[8] Suzuki T Y, Suzuki H, Currell F J, Ohtani S, Takayanagi T and Wakiya K 1996 Measurements of cross sections and oscillator strengths by electron impact for the 5d and 7s levels of xe *Phys. Rev.* A **53** 4138–44

[9] Suzuki T Y, Suzuki H, Ohtani S, Takayanagi T and Okada K 2007 Asymptotic behavior of apparent generalized oscillator strengths for optically forbidden transitions in rare-gas atoms *Phys. Rev.* A **75** 032705

[10] Amusia M Y, Chernysheva L V, Felfli Z and Msezane A Z 2003 Determination of discrete transition multipolarity using the generalized oscillator strength *Phys. Rev.* A **67** 022703

[11] Amusia M Y, Chernysheva L V, Felfli Z and Msezane A Z 2007 Octupole contributions to the generalized oscillator strengths of discrete dipole transitions in noble-gas atoms *Phys. Rev.* A **75** 062703

[12] Amusia M Y 2007 Fast electron and x-ray scattering as a tool to study target's structure *J. Electron Spectrosc. Relat. Phenom.* **159** 81–90